Photochemical & Photobiological Sciences

PAPER

Cite this: *Photochem. Photobiol. Sci.*, 2016, **15**, 1029

# Effect of substitution on the ultrafast deactivation of the excited state of benzo[*b*]thiophene-arylamines†

J. Pina,*[a] M.-J. R. P. Queiroz[b] and J. Seixas de Melo[a]

Received 6th May 2016,
Accepted 29th June 2016

DOI: 10.1039/c6pp00140h

www.rsc.org/pps

A complete and systematic study of the spectroscopic and photophysical properties of five novel diarylamines in the benzo[*b*]thiophene series (oligoanilines) was performed in solution at room (293 K) and low (77 K) temperature. The title compounds resulting from the link between one aniline unit with a benzo[*b*]-thiophene unit (with two different methyl and methoxy substitution) were characterized using steady-state absorption, fluorescence and phosphorescence spectroscopy, as well as femto- to nano-second time resolved spectroscopies. The study involved the determination of the absorption, emission and triplet–triplet absorption together with all relevant quantum yields (fluorescence, phosphorescence, intersystem crossing, internal conversion and singlet oxygen yields), excited state lifetimes and the overall set of deactivation rate constants ($k_F$, $k_{IC}$ and $k_{ISC}$). This study was further complemented with theoretical calculations, namely with the determination of the optimized ground-state molecular geometries for the diarylamines together with the prediction of the lowest vertical one-electron excitation energy and the relevant molecular orbital contours using DFT calculations. The DFT results were found to corroborate the observed charge-transfer character of the singlet excited state. The experimental results showed that the radiationless decay processes (internal conversion and intersystem-crossing) constitute the main excited state deactivation pathways and that substitution with methyl and methoxy groups induces significant changes in the spectroscopic and photophysical behaviour of these compounds. This was also corroborated by the femtosecond transient absorption study, where it was found that the ultrafast dynamics of the diarylamines was best described by a sequential model featuring fast solvent relaxation followed by conformational relaxation to a more planar excited state, from where singlet excited state deactivation occurs through internal conversion and competitive intersystem crossing (the latter giving rise to the formation of long lived triplet states). The high singlet oxygen quantum yield values obtained suggest that the triplet state is involved in the photodegradation processes of these compounds.

## Introduction

Due to their luminescent properties benzo[*b*]thiophenes are relevant heterocyclic systems, both as biologically active molecules[1,2] and as sensors.[3,4] On the other hand aniline and polyaniline are in the genesis of all the chemical industry and in particular of the dye industry.[5,6] Polyaniline, due to its high electrical conductivity is one of the most investigated organic conjugated polymers and although in the past most of the studies were associated to polyaniline, in the present the tendency is more devoted to oligomeric materials derived from polyalinine.[7] This is because these materials are easily processable and usually their physicochemical properties can be improved by simple modification. For the improvement of their electronic properties, oligoanilines can be functionalized by adding covalently bonded side chain groups. Electron-acceptor groups affect the LUMO orbital (lowering the LUMO energy) and electron-donor group side chains instead affect the HOMO orbital thus changing the $\Delta E$ HOMO–LUMO.[7] In this work the benzo[*b*]thiophene unit was linked to aniline through the benzene or the thiophene rings.

In recent years the antioxidant properties and more specifically the radical scavenger activity of several substituted benzo-[*b*]thiophenes-arylamines derivatives have been investigated.[2,8,9] Some compounds have shown a good antioxidant activity, which was seen to be dependent of the type of substituents and their position either on the benzene moiety or on the thiophene ring. While the rich excited state properties of phenylamines and condensed ring systems of alternating benzenes and thiophenes have been extensively studied,[10–12]

[a]*Coimbra Chemistry Center, Department of Chemistry, University of Coimbra, 3004-535 Coimbra, Portugal. E-mail: jpina@qui.uc.pt*
[b]*Department of Chemistry, University of Minho, 4700-320 Braga, Portugal*
†Electronic supplementary information (ESI) available. See DOI: 10.1039/c6pp00140h

oligoanilines involving benzo[*b*]thiophene and arylamine units have been poorly explored and investigated.

The present work aimed at providing a photophysical characterization of a series of diarylamines derived from aniline and functionalized with a benzo[*b*]thiophene unit. The choice of these groups was due to the fact that aniline is the oligomeric precursor of the well-known polyaniline which is an important organic conjugated polymer.[9,13] The conducting properties of polyaniline derive from its great stability and easy modification by changing its oxidation state or protonation degree.[12,14]

A comprehensive photophysical characterization of methyl- and methoxy-substituted diarylamines in the benzo[*b*]thiophene series, in particular the excited state properties from the μs to the fs time domains is obtained. Moreover, to the best of our knowledge this is the first comprehensive photophysical characterization of oligoanilines, including femtosecond (fs) transient absorption.

## Experimental

The benzo[*b*]thiophene-arylamine derivatives were synthesized as described elsewhere.[15–17] For the spectral and photophysical determinations, the solvents used were of spectroscopic or equivalent grade. Ethanol was previously dried over CaO and then distilled. Absorption spectra were obtained on a Shimadzu UV-2100 spectrometer. Fluorescence and phosphorescence experiments were recorded with a Horiba Jovin Yvon Fluorolog 3-2.2 spectrometer (the latter using the D1934 unit). Fluorescence and phosphorescence spectra were corrected for the wavelength response of the system. The fluorescence quantum yields ($\phi_F$) of the oligoanilines at 293 K were determined using 2,2′-bithiophene in ethanol ($\phi_F$ = 0.014)[18] as standard. The fluorescence quantum yields at 77 K were obtained by comparison with the spectrum at 293 K run under the same experimental conditions. The following eqn (1) was then applied,[19]

$$\phi_F^{77\,K} = \frac{\int I(\lambda)^{77\,K} d\lambda}{\int I(\lambda)^{293\,K} d\lambda} \cdot \phi_F^{293\,K} f_c \quad (1)$$

where $\int I(\lambda)^x d\lambda$ is the integrated area under the emission of the sample at 77 K and 293 K, $\phi_F^{293\ K}$ is the fluorescence quantum yield at 293 K and $f_c$ is the factor that considers the "shrinkage" of the solvent (volume) upon cooling, given by $V_{77\ K}/V_{293\ K}$ = 0.8.

The phosphorescence quantum yield was measured using benzophenone in ethanol ($\phi_{Ph}$ = 0.84) as standard.[19] Fluorescence decays were measured using a home-built TCSPC apparatus as described elsewhere.[20,21] The fluorescence decays were analyzed using the method of modulating functions implemented by Striker.[22,23]

The ground state molecular geometry was optimized using the density functional theory (DFT) by means of the Gaussian 09 program,[24] under B3LYP/6-31G(d,p) level.[25,26]

Optimal geometries were determined on isolated entities in a vacuum and no conformation restrictions were imposed. For the resulting optimized geometries time dependent DFT calculations (using the same functional and basis set as those of the previous calculations) were performed to predict the vertical electronic excitation energies. Molecular orbital contours were plotted using GaussView 5.0.8.

Triplet–singlet difference absorption spectra and yields were obtained using an Applied Photophysics laser flash photolysis equipment pumped by a Nd:YAG (Spectra Physics) laser with excitation wavelength at 266 nm as described elsewhere.[21] The transient spectra were obtained by monitoring the optical density change at 5–10 nm intervals, averaging at least 10 decays at each wavelength. The triplet molar absorption coefficients were determined by the singlet depletion technique[27] and the $\phi_T$ value was obtained by comparing the ΔOD at 410 nm of an ethanol solution of naphthalene ($\phi_T$ = 0.80,[19] $\varepsilon_T$ = 40 000 $M^{-1}$ $cm^{-1}$)[18] optically matched at the laser wavelength with the compound solution. Singlet oxygen yields were measured at the FRRF (Daresbury laboratories), by direct measurement of the phosphorescence at 1270 nm followed by the irradiation of an aerated solution of the samples in cyclohexane with excitation at 266 nm from a Nd:YAG laser with a setup described elsewhere.[28] Biphenyl in cyclohexane ($\phi_\Delta$ = 0.73) was used as standard.[29]

The experimental setup for ultrafast spectroscopic and kinetic measurements was described elsewhere[30] and consists of a broadband (350–1600 nm) HELIOS pump–probe femtosecond transient absorption spectrometer from Ultrafast Systems, equipped with an amplified femtosecond Spectra-Physics Solstice-100F laser (displaying a pulse width of 128 fs and 1 kHz repetition rate) coupled with a Spectra-Physics TOPAS Prime F optical parametric amplifier (195–22 000 nm) for pulse pump generation. Probe light in the UV range was generated by passing a small portion of the 795 nm light from the Solstice-100F laser through a computerized optical delay (with a time window up to 8 ns) and focusing in a vertical translating $CaF_2$ crystal to generate white-light continuum (350–750 nm). All measurements were obtained in a 2 mm quartz cuvette with absorptions lower than 0.3 at the pump excitation wavelength. The instrumental response function of the system was assumed to be equal to that of the pump–probe cross correlation determined from the measurement of the instantaneous stimulated Raman signal from the pure solvent (in a 2 mm cuvette). Typical values for the IRF of the system were found to be better than 250 fs. To avoid photodegradation the solutions were stirred during the experiments or in movement using a motorized translating sample holder. Transient absorption data were analyzed using the Surface Xplorer PRO program from Ultrafast Systems and the global analysis of the data (from which the lifetimes and decay associated spectra, DAS, of the observed transients were obtained) was performed using Glotaran software.[31]

## Results and discussion

The structures and acronyms of the studied compounds are depicted in Scheme 1. The fundamental structure consists of a

 

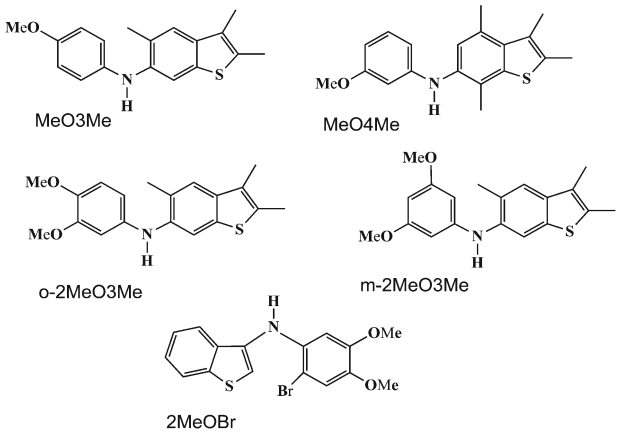


**Scheme 1** Structures and acronyms of the investigated benzo[*b*]thiophene-arylamines.

benzo[*b*]thiophene-arylamine (oligoaniline) with different levels and positions of methoxy and methyl substitution.[15,16] In one of the compounds (2MeOBr)[17] aniline is linked to the benzo[*b*]thiophene unit through the thiophene unit whereas in all the other compounds the link is between aniline and the benzene ring (of the benzothiophene unit).

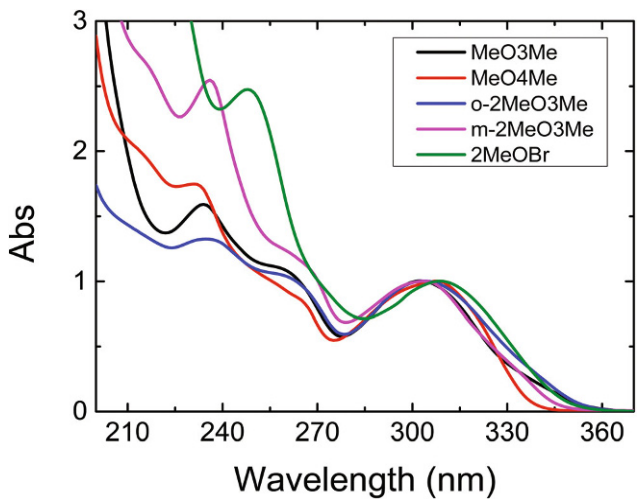


**Fig. 1** Normalized absorption spectra for the oligoanilines in ethanol solution at 293 K.

### Absorption and fluorescence

Fig. 1 presents the absorption spectra of the investigated samples at room temperature in ethanol solution. In general, the spectra are devoid of vibronic structure and present similar wavelength maxima and molar extinction coefficients (in the 12 600–17 600 $M^{-1}$ $cm^{-1}$ range, thus pointing to the π–π* character of the lowest lying singlet excited state), see Table 1 and Fig. 1. The exception occurs with 2MeOBr where a red-shift of *ca*. 6 nm is observed when compared to the other investigated compounds (Table 1). The red-shift of 2MeOBr can be explained by the increase in electronegativity induced by the presence of the bromine atom that promotes a bathochromic shift in the lowest lying π–π* transition band.[32]

The fluorescence emission spectra of the compounds in ethanol at room temperature (293 K) and low temperature (77 K) are presented in Fig. 2. In agreement to what was observed in the absorption spectra at 293 K the fluorescence emission spectra are devoid of vibronic structure. Noteworthy are the large Stokes-shift values (which are found to be in the 4404–10 682 $cm^{-1}$ range) thus pointing to the charge transfer (CT) character of the fluorescence emission band in agreement to what was reported for aminodiphenylamine derivatives.[10]

For the present compounds is also noteworthy the high Stokes-shift value (10 682 $cm^{-1}$) found for the *ortho*-methoxy substituted derivative thus showing that this substitution (electron acceptor units) increases the bathochromic shift of the CT fluorescence band (through extension of the electronic delocalization).

Upon going to low temperature (ethanol glasses at 77 K), in general, a vibronically resolved long wavelength phosphorescence emission band (see Fig. 2 and S2 in ESI†) is observed in addition to a significantly blue-shifted unstructured fluorescence emission band (by 18–76 nm, when compared to the spectra at 293 K). The exception was for the 2MeOBr derivative where a significant increase in the vibronic structure and a negligible 4 nm blue-shift of the fluorescence emission band was observed in addition to the long wavelength phosphorescence emission band (see Fig. 2 and Table 1).

**Table 1** Spectroscopic data (absorption, fluorescence and phosphorescence emission, triplet absorption maxima, molar singlet and triplet extinction coefficients, $\varepsilon_S$ and $\varepsilon_T$, Stokes-shift, $\Delta_{SS}$, together with the singlet and triplet energies, $E_S$ and $E_T$) for the investigated oligoanilines in ethanol solution at 293 K and 77 K. The underlined values represent the maxima in the spectra

| Compound | $\lambda_{max}^{S_0\rightarrow S_n}$ (nm) 293 K | $\lambda_{max}^{S_1\rightarrow S_0}$ (nm) 293 K | $\lambda_{max}^{S_1\rightarrow S_0}$ (nm) 77 K | $\lambda_{max}^{T_1\rightarrow S_0}$ (nm) 77 K | $\lambda_{max}^{T_1\rightarrow T_n}$ (nm) 293 K | $\varepsilon_S$ ($M^{-1}$ $cm^{-1}$) 293 K | $\varepsilon_T$ ($M^{-1}$ $cm^{-1}$) 293 K | $E_S$ [a] (eV) 293 K | $E_T$ [b] (eV) 293 K | $\Delta_{SS}$ $cm^{-1}$ 293 K |
|---|---|---|---|---|---|---|---|---|---|---|
| 2MeOBr | 309 | 364 | 342, 360, 380 | 490, 520 | 465 | — | — | 3.66 | 2.69 | 4890 |
| MeO3Me | 303 | 417 | 368 | 471, 503 | 410, 526 | 16 500 | 48 000 | 3.50 | 2.76 | 9022 |
| MeO4Me | 307 | 355 | 337 | 471, 498 | 410, 515 | 16 400 | 18 300 | 3.73 | 2.79 | 4404 |
| *o*-2MeO3Me | 303 | 448 | 372 | 471, 502 | 380, 548 | 17 600 | 44 100 | 3.49 | 2.76 | 10 682 |
| *m*-2MeO3Me | 303 | 370 | 348 | 466, 497 | 540 | 12 600 | 24 200 | 3.65 | 2.78 | 5976 |

[a] Obtained from the intersection between the lowest energy absorption band and the fluorescence emission band. [b] Obtained from the onset of the phosphorescence emission band.

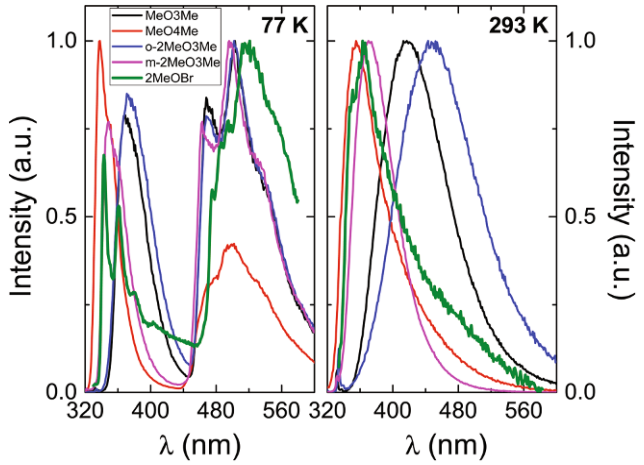


Fig. 2 Fluorescence emission spectra for the oligoanilines in ethanol at low (77 K) and room temperature (293 K). At 77 K the phosphorescence emission spectra (band at 440–580 nm) is obtained together with the low temperature fluorescence emission band (320–450 nm).

The fluorescence quantum yields at 293 K (Table 2) are in general low (in agreement to the value found for benzothiophene, $\phi_F$ = 0.019 in ethanol),[11] ranging from 0.0027 to 0.072; however, these values double at 77 K, which can be partially explained by the dominance of the radiative over the non-radiative processes when the temperature is decreased.[32] In fact, at low temperatures the torsional degree of freedom between the two moieties (diarylamine and benzothiophene) is reduced, which potentially leads to a decrease of the energy dissipation through the internal $S_1 \rightsquigarrow S_0$ deactivation channel (minimizing the loose bolt effect[33]).

The fluorescence lifetimes obtained in ethanol were found to be single exponential for all compounds (Fig. 3 and Table 2), in agreement to what was reported for benzothiophene, $\tau_F$ = 0.28 ns, and for aminodiphenylamine derivatives ($\tau_F$ in the 0.9–3.8 ns range).[10,11] With the exception of 2MeOBr, which displays a short lifetime, 39 ps, the remaining lifetimes are in the 1.8–2.5 ns range (see Table 2).

### Theoretical calculations

To further investigate the electronic properties of the investigated compounds the ground state optimized geometry structures and the relevant HOMO and LUMO energy levels, together with their electron density distribution surface plots were obtained at the DFT/B3LYP/6-31G(d,p) level. Frequency

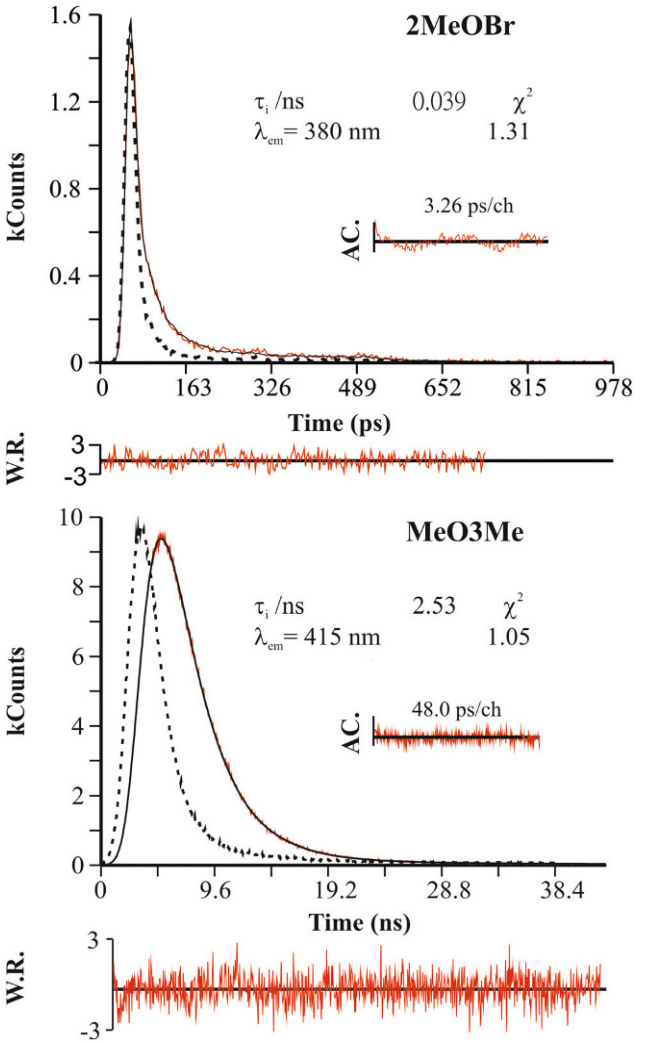


Fig. 3 Room-temperature fluorescence decays for compounds 2MeOBr and MeO3Me in ethanol solution. For a better judgment of the quality of the fit, weighted residuals (W.R.), autocorrelation function (A.C.) and $\chi^2$ values are also presented. The dashed lines in the decays are the instrumental response function.

Table 2 Photophysical properties including quantum yields (fluorescence, $\phi_F$, phosphorescence, $\phi_{Ph}$, internal conversion, $\phi_{IC}$, triplet formation, $\phi_T$, and sensitized singlet oxygen, $\phi_\Delta$), lifetimes ($\tau_F$, $\tau_{Ph}$, $\tau_T$) and rate constants ($k_F$, $k_{NR}$, $k_{IC}$ and $k_{ISC}$) for the investigated compounds in ethanol solution at 293 K and 77 K

| Compound | $\phi_F$ 293 K | $\phi_F$ 77 K | $\tau_F$ (ns) 293 K | $\phi_{Ph}$ 77 K | $\tau_{Ph}$ (s) 77 K | $\phi_T$ 293 K | $\phi_\Delta$ [a] 293 K | $\tau_T$ (μs) 293 K | $\phi_{IC}$ [b] 293 K | $k_{NR}$ [b] ($ns^{-1}$) 293 K | $k_F$ [b] ($ns^{-1}$) 293 K | $k_{IC}$ [b] ($ns^{-1}$) 293 K | $k_{ISC}$ [b] ($ns^{-1}$) 293 K |
|---|---|---|---|---|---|---|---|---|---|---|---|---|---|
| 2MeOBr | 0.0027 | 0.014 | 0.039 | 0.17 | 0.036 | — | 0.04 | 21 | — | 25.6 | 0.069 | — | — |
| MeO3Me | 0.059 | 0.12 | 2.53 | 0.30 | 0.18 | 0.20 | 0.28 | 8 | 0.74 | 0.37 | 0.023 | 0.29 | 0.079 |
| MeO4Me | 0.038 | 0.19 | 1.88 | 0.15 | 0.23 | 0.28 | 0.29 | 5 | 0.68 | 0.51 | 0.020 | 0.36 | 0.14 |
| *o*-2MeO3Me | 0.033 | 0.15 | 2.31 | 0.37 | 0.17 | 0.38 | 0.33 | 43 | 0.59 | 0.42 | 0.014 | 0.25 | 0.16 |
| *m*-2MeO3Me | 0.072 | 0.096 | 1.92 | 0.29 | 0.19 | 0.27 | 0.30 | 15 | 0.63 | 0.48 | 0.038 | 0.33 | 0.14 |

[a] Values obtained in cyclohexane. [b] $k_F = \frac{\phi_F}{\tau_F}$; $k_{NR} = \frac{1-\phi_F}{\tau_F}$; $k_{IC} = \frac{1-\phi_F-\phi_T}{\tau_F}$; $k_{ISC} = \frac{\phi_T}{\tau_F}$; $\phi_{IC} = 1-\phi_F-\phi_T$.

analyses for each compound were also computed and did not yield any imaginary frequencies, indicating that the structure of each molecule corresponds to at least a local minimum on the potential energy surface. The geometry optimization for the investigated compound revealed that the phenyl moieties (in the aniline chromophores) are non-planar with respect to the plane formed by the benzo[*b*]thiophene unit, displaying dihedral angles of 45°, 178°, 41°, 30° and 67° for MeO3Me, MeO4Me, *o*-2MeO3Me, *m*-2MeO3Me and 2MeOBr, respectively (see Fig. 4 and S1 in ESI†).

Since the time-dependent density functional theory (TD-DFT) approach is known to accurately predict the structural and optical properties of sulfur containing compounds[34,35] this method was used at the B3LYP/6-31G(d,p) level on the previously optimized ground-state molecular geometries to obtain the vertical excitation energies, oscillator strengths ($f$) and excited state compositions in terms of excitations between the occupied and virtual orbitals for the investigated compounds. For the diarylamines MeO3Me and *o*-2MeO3Me the observed lowest energy absorption bands are associated to the predicted $S_0 \rightarrow S_1$ [312 nm ($f$ = 0.2791) for MeO3Me and 313 nm ($f$ = 0.3996) for *o*-2MeO3Me] and $S_0 \rightarrow S_2$ transitions [305 nm ($f$ = 0.2573) for MeO3Me and 298 nm ($f$ = 0.1679) for *o*-2MeO3Me], Table S1 in ESI.† In general these transitions display contributions from the HOMO → LUMO and HOMO → LUMO+1 orbitals. It is noteworthy that for the $S_0 \rightarrow S_1$ transition the major contribution arises from the HOMO → LUMO orbitals (73% for MeO3Me and 89% for *o*-2MeO3Me) while for the $S_0 \rightarrow S_2$ transitions the HOMO → LUMO+1 orbitals present higher contribution (74% for MeO3Me and 86% in the case of *o*-2MeO3Me).

In the case of the diarylamines MeO4Me, *m*-2MeO3Me and 2MeOBr the lowest energy transitions are associated to the $S_0$–$S_1$ transition [predicted at 303 nm ($f$ = 0.2792) for MeO4Me, 307 nm ($f$ = 0.4623) for *m*-2MeO3Me and 302 nm ($f$ = 0.0946) for 2MeOBr], displaying predominantly contribution from the HOMO → LUMO orbital (>91%), see Table S1 in ESI.† Although for aromatic donor–acceptor systems, it is known that the TD-DFT approach overestimates the absorption wavelengths of CT-type transitions (with errors of up to 1 eV),[35] in our case the predicted transitions are in good agreement with the experimental values (deviations in the 0.05–0.13 eV range), thus giving additional support for the calculated molecular geometries (Table S1 in ESI†). In addition, the non-negligible oscillator strength values predicted for the $S_0 \rightarrow S_1$ and $S_0 \rightarrow S_2$ transitions give further support for the symmetry allowed character, π–π*, of the observed lowest energy absorption bands.

The molecular orbital contours (Fig. 4) show that the densities of the HOMO orbitals are, in general, spread over the entire molecules, while the LUMO shows a decrease in the electron density on the aniline moieties and a concomitant increase in the benzo[*b*]thiophene units. Moreover, the electronic delocalization in the LUMO orbitals gives further support for the occurrence of CT in the singlet excited state.

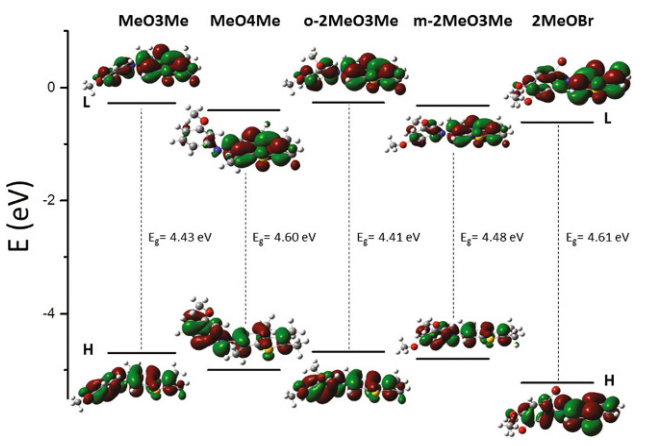


**Fig. 4** DFT//B3LYP/6-31G(d,p) optimized ground-state geometry together with the frontier molecular orbital energy levels and the relevant electronic density contours for the investigated compounds. Also displayed are the predicted optical band gap energy values, $E_g$.

## Triplet-state

In contrast to the observed behaviour found for diphenylamines, where no phosphorescence emission is observed, fused oligothiophene derivatives are known to display phosphorescence.[10,11,36] The phosphorescence emission spectra of the oligoanilines are shown in Fig. 2 (and Fig. S2 in ESI†). The phosphorescence quantum yields ($\phi_{Ph}$) are fairly high, denoting that this process is one of the main channels for the deactivation of the excited state (see Table 2). The decrease in the vibronic structure and the red-shift of the phosphorescence emission spectra of the oligoanilines when compared to benzothiophene indicates that an electronic conjugative interaction involving the benzothiophene and the arylamine units is present in the triplet state; additional support to this conclusion comes from the decrease in the $\phi_{Ph}$ values ($\phi_{Ph}$ in the 0.15–0.37 range *vs.* 0.42 for benzothiophene) and phosphorescence lifetimes ($\tau_{Ph}$ in the 0.036–0.23 s *vs.* 0.32 s).[11]

The triplet states of these compounds were also investigated by nanosecond transient absorption, ns-TA, (in the nanosecond–microsecond time regime). The transient triplet–triplet absorption spectra for these compounds are broad (see Fig. S3 in ESI†), which suggests a high delocalization of the triplet excited state probably due to the increase in the spin–orbit coupling promoted by the π electrons of the oxygen atoms and supports the high degree of electronic interactions involving the benzothiophene (triplet absorption maxima at 430 nm and $\tau_T$ = 17.3 μs)[11] and the arylamines units in the triplet state.

From the observation of data in Table 1 it can be seen that the triplet absorption maxima and extinction coefficients values ($\varepsilon_T$) are, within the experimental error, approximately identical for all the studied compounds, thus showing that no influence is promoted by the number and position of methyl and methoxy groups respectively. However, the same does not happen with fluorescence where the emission maximum at 293 K (and 77 K) now depends on the position and number of substituents. For example methoxy disubstitution at the *ortho* position of the benzenic ring (aniline moiety), *o*-2MeO3Me,

leads to a more red-shifted emission wavelength maxima, whereas in the case of the *meta* substitution, *m*-2MeO3Me, it leads to a blue shift of the emission maximum, see Table 1. While for 2MeOBr, the introduction of a bromine group in addition to a (single) methoxy group, MeO4Me, leads to the shortest wavelength emission maximum of the series of compounds studied.

Moreover the relatively constant values for the radiative rate constants ($k_F \approx 0.01$–$0.07$ ns$^{-1}$), together with the relatively high molar singlet extinction coefficients ($\varepsilon_S > 12\,600$ M$^{-1}$ cm$^{-1}$) obtained from the lowest energy transition, points to an allowed π,π* character of the lowest lying singlet excited state. In addition, the singlet–triplet energy splitting, $\Delta E_{ST}$, values found in the 0.74–0.97 eV range [$\Delta E_{ST}(\pi$–$\pi^*) > 0.62$ eV], together with the phosphorescence lifetime values also points to a π–π* character of the triplet excited state.[37,38]

### Singlet oxygen sensitization

Singlet oxygen formation quantum yields were obtained following photolysis of aerated cyclohexane solutions of the oligoanilines. Excitations with laser pulses of a Nd:YAG laser (266 nm) lead to the characteristic phosphorescence emission of singlet oxygen at ≈1270 nm. The $\phi_\Delta$ values were determined by plotting the initial phosphorescence intensity (at 1270 nm) as a function of the laser dose and comparing the slope with that obtained with biphenyl in cyclohexane as standard (see Experimental for further details). From Table 2 it can be seen that the singlet oxygen formation yields are roughly constant with values lying between 0.28 and 0.33 with the exception of 2MeOBr where this value is significantly lower, $\phi_\Delta \approx 0.04$ (see Table 2). It is also worth noting that they are also very close to the quantum yields for triplet formation, providing support for the latter values, and indicating that the efficiency of triplet energy transfer to produce singlet oxygen ($S_\Delta = \phi_\Delta/\phi_T$) is very close or nearly 1, suggesting very efficient energy transfer from the oligoanilines to ground-state triplet molecular oxygen. For 2MeOBr however, if we consider that in general $\phi_T \geq \phi_{Ph} = 0.17$ (see Table 2), the lower $\phi_\Delta$ value suggests that the singlet oxygen sensitization efficiency is low, $S_\Delta \leq 0.24$. Analysis of Table 2 shows that for compound MeO3Me the value found for $\phi_\Delta$ is in agreement with $\phi_{Ph}$, thus suggesting that the $\phi_T$ value is underestimated.

In general the dominance of the radiationless deactivation pathways (internal conversion, $\phi_{IC}$, and intersystem-crossing, $\phi_T$) and in particular the existence of a competitive singlet-to-triplet intersystem crossing suggests the heavy-atom effect (due to the presence of the sulfur atom in the benzothiophene unit) to be operative.

### Femtosecond transient absorption (fs-TA)

The time-resolved transient absorption spectra for the investigated compounds in aerated ethanol solution were measured in the 350–750 nm range with excitation at 310 nm and collected within a 7.5 ns time-window, see Fig. 5 and S4 in ESI.† The fs-TA data show that, in general, the spectra are dominated by positive broad transient absorption bands (in the 350–650 nm range) that clearly result from the convolution of two transient absorption spectral features. Immediately after excitation, a broad transient absorption band appears that, in agreement to what was observed for benzothiophene,[11] contributes to the excited state absorption (ESA) of the investigated compounds. As the delay time increases this band disappears and a new band arises (corroborated by the presence of isosbestic points in the transient absorption spectra, see Fig. 5 and S4 in ESI†), which does not decay completely up to the longest delay time measured (Fig. 6B and S5–7 in ESI†). This observation points to the occurrence of a direct dynamical conversion from one state into another state. Although these characteristic bands overlap with each other to a certain extent, due to the spectral resemblance of the bands observed at higher delay times in the fs-TA setup with the triplet–triplet absorption spectra obtained by ns-TA (see Fig. 5 and S4 in ESI†), together with their long lived nature, these are assigned to the $T_1 \rightarrow T_n$ ESA, following intersystem crossing.

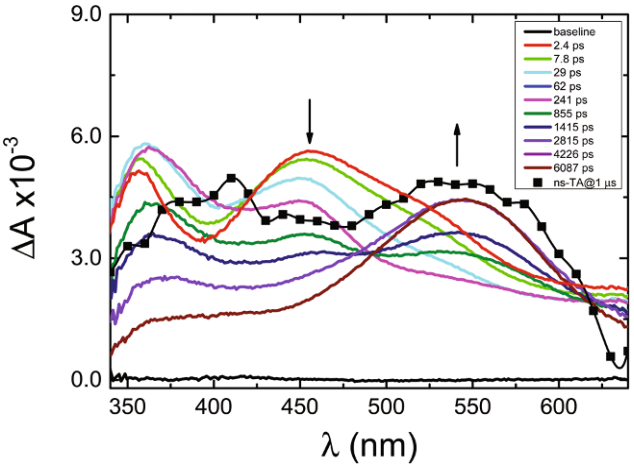


**Fig. 5** Time-resolved transient absorption data (collected in the fs-TA and in ns-TA spectrometers) for MeO3Me in ethanol solution at room temperature. The vertical arrows indicate the direction of the absorbance evolution.

Nevertheless to describe properly the observed dynamics, global fit analysis (using a sequential model) of all of the kinetics in the 350–650 nm region was performed with singular value decomposition (SVD). The best-fit results together with the decay associated spectra (DAS), concentration profiles of the time constants and representative kinetic traces of the characteristic transient absorption data are presented in Table 3, Fig. 6 and S5–7.† With the exception of 2MeOBr, in general, the experimental traces over the whole spectra-temporal range are well fitted with the sum of four exponentials (Table 3 and Fig. 6 and S5–7†): (i) a first fast decay transient with values of 0.242 ps for *m*-2MeO3Me and in the 6.6–14 ps range for the oligoanilines MeO3Me, MeO4Me and *o*-2MeO3Me; (ii) a second one with values in the 50–110 ps range; (iii) a third one with values ranging from 695 ps to 1621 ps; (iv) and a long lived transient associated to the triplet state decay. For the latter time constant, since the kinetic

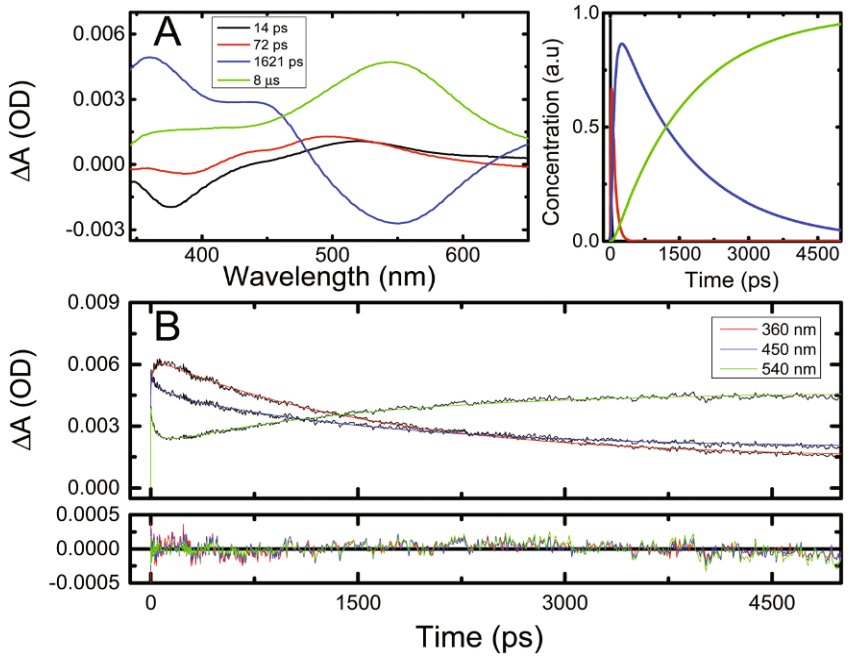


**Fig. 6** (A) Decay associated spectra (DAS) of the four time constants extracted from the time-resolved femtosecond transient absorption data ($\lambda_{exc}$ = 310 nm) after SVD/global analysis together with the concentration profiles of the time constants for MeO3Me in ethanol solution at 293 K; (B) representative kinetic traces with fits from the global analysis of the transient absorption data. For a better judgment of the quality of the fits the residuals are also presented.

**Table 3** Results of the global fit analysis (lifetimes, $\tau_i$, and normalized pre-exponential factors, $a_{ij}$) obtained from the ultrafast time-resolved transient absorption data of the investigated oligoanilines in ethanol solution at 293 K

| Compound | $\lambda$ (nm) | $\tau_1$ (ps) | $\tau_2$ (ps) | $\tau_3$ (ps) | $\tau_4$ (μs) | $a_{i1}$ | $a_{i2}$ | $a_{i3}$ | $a_{i4}$ |
|---|---|---|---|---|---|---|---|---|---|
| 2MeOBr | 425 | 1.6 | | 39 | 21 | 0.36 | | 0.50 | 0.14 |
| | 490 | | | | | 0.24 | | 0.65 | 0.11 |
| MeO3Me | 360 | 14 | 72 | 1621 | 8 | −0.22 | −0.03 | 0.78 | 0.22 |
| | 450 | | | | | 0.03 | 0.12 | 0.50 | 0.35 |
| | 540 | | | | | 0.14 | 0.14 | −0.40 | 0.72 |
| MeO4Me | 360 | 19 | 76 | 695 | 5 | −0.21 | −0.42 | 0.69 | 0.31 |
| | 450 | | | | | 0.04 | 0.44 | 0.20 | 0.33 |
| | 515 | | | | | 0.21 | 0.01 | −0.17 | 0.77 |
| *o*-2MeO3Me | 360 | 6.6 | 50 | 1429 | 43 | −0.20 | −0.06 | 0.86 | 0.14 |
| | 450 | | | | | 0.28 | 0.14 | 0.41 | 0.18 |
| | 550 | | | | | 0.31 | 0.12 | −0.24 | 0.57 |
| *m*-2MeO3Me | 460 | 0.242 | 110 | 814 | 15 | 0.44 | 0.18 | 0.04 | 0.34 |
| | 540 | | | | | 0.23 | 0.03 | −0.47 | 0.74 |

traces associated to the triplet state could not be fitted within the monitoring time-window (see Fig. 6 and S5–7†), the long lived components were fixed in the analysis to their respective triplet lifetimes obtained by ns-TA, 5–43 μs, (Table 2).

The fast decay components observed, with values of 0.242 ps for *m*-2MeO3Me and in the 6.6–14 ps range for the oligoanilines MeO3Me, MeO4Me and *o*-2MeO3Me are consistent with the solvation dynamics times previously reported for coumarin C153 in ethanol.[39] The occurrence of fast vibrational relaxation was discarded since similar fast transient times were obtained when excitation was performed at lower energies (in the 0–0 transition absorption band). Thus, the 0.242 ps found for *m*-2MeO3Me can be related to the fast inertial solvation time (0.29–1.4 ps), while the values in the 6.6–14 ps range found for MeO3Me, MeO4Me and *o*-2MeO3Me can be assigned to the diffusional solvation component observed in ethanol (16 ps).[39]

To further investigate the nature of the remaining two decay components the transient absorption spectra for MeO3Me in the more viscous methanol : glycerol (50 : 50 v/v) mixture were obtained. Similar transient absorption spectral features to those found in ethanol were observed in the methanol : glycerol mixture (see Fig. 5 and S8 in ESI†). Again the results of the global analysis showed that the data is best

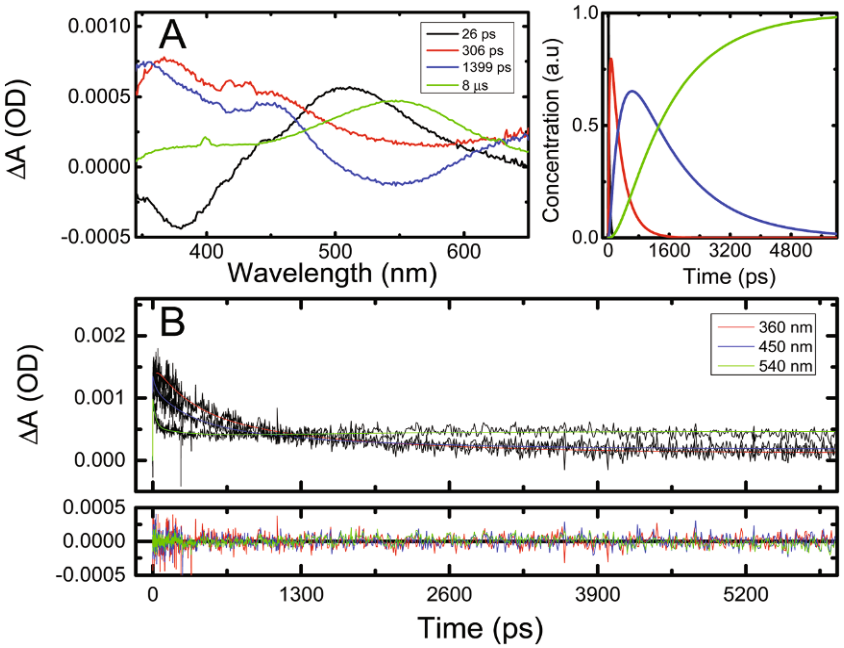


**Fig. 7** (A) Decay associated spectra (DAS) of the four time constants extracted from the time-resolved femtosecond transient absorption data ($\lambda_{exc}$ = 315 nm) after SVD/global analysis together with the concentration profiles of the time constants for MeO3Me in a methanol : glycerol (50 : 50 v/v) mixture at 293 K; (B) representative kinetic traces with fits from the global analysis of the transient absorption data. The residuals are also presented for a better judgment of the quality of the fits.

fitted with four components (Fig. 7). It is noteworthy the increase of the two fastest decay components with the solvent viscosity (from 14 ps in ethanol, to 26 ps in the methanol : glycerol mixture and from 72 ps to 306 ps, respectively), thus showing that these are solvent (diffusion) controlled processes. In the case of the first decay component this behavior supports the assignment of the fast transients to solvent relaxation. However, for the second fast transients (50–110 ps), in agreement with the behavior found for aminodiphenylamine derivatives, these lifetimes are better associated to conformational relaxation.[10] While the transient lifetimes in the 695–1621 ps range are ascribed to the decay of the fully relaxed (more planar) singlet excited state. The lower values found for the latter transient lifetimes when compared with the fluorescence lifetimes obtained from time correlated single photon counting (values in the 1880–2530 ps range), gives further support for the observed prevalence of the radiationless processes in the singlet excited state deactivation of the investigated compounds (with the fluorescence rate constant, $k_F$, one order of magnitude lower than the non-radiative rate constant, $k_{NR}$, see Table 2). Indeed, from the overall set of photophysical parameters including quantum yields and rate constants presented in Table 2 it can be seen that the radiationless deactivation channels ($\phi_{IC} + \phi_T$) are the main excited state deactivation pathways. Moreover it can also be seen that the two radiationless rate constants, $k_{IC}$ and $k_{ISC}$ have approximately the same values thus constituting competitive deactivation pathways of the singlet excited state of these compounds.

Thus the excited state dynamics of the investigated compounds can be described through a series of sequential relaxation steps (see Fig. S10 in ESI†): (i) upon photoexcitation, molecules that are initially in twisted ground states[10] are vertically excited to a Franck–Condon state, FC; (ii) which undergoes fast solvent relaxation to a locally excited state, LE; (iii) that further relaxes through conformational relaxation to a more planar excited state;[10] (iv) which, then gives rise to the formation of the long lived triplet states. The observed negative amplitude values observed in the DAS of the 695–1621 ps time constants in the wavelength region where the $T_1$–$T_n$ ESA occurs, along with the distinct rise of the long-lived DAS kinetics (Fig. 6 and S5–7 in ESI†) supports the triplet state being formed at the expenses of the more planar excited state. In addition the measured ISC rate constants obtained by the reciprocal of the third DAS values, in the 0.62–1.4 $ns^{-1}$ range, are in good agreement with the values estimated indirectly in Table 2 using the $k_{ISC} = \phi_T/\tau_F$ relation, thus giving support for the latter values.

For 2MeOBr the best fit to the data was found using a total of three components from which the corresponding DAS along with the time evolution of each component are shown in Fig. S9.† In this case a short transient component of 1.6 ps together with a 39 ps intermediary decay time and a long-lived transient (not decaying within the fs-TA setup time-window) were found in the analysis (Table 3). Although the time-resolved spectra for 2MeOBr is dominated by broad and significantly overlapped transient absorption bands the strong resemblance in shape and maxima between the spectra

collected at latter delay times and the triplet–triplet absorption spectra obtained by ns-TA, together with the long lived nature makes us assign this transient to the $T_1 \rightarrow T_n$ ESA (see Fig. S4 and S9 in ESI†). Thus in the global analysis this transient lifetime was fixed to the triplet lifetime obtained by ns-TA (21 μs, Table 2). Moreover the global analysis suggests that the initially formed excited state (FC state) undergoes rapid solvent relaxation, 1.6 ps (in agreement to the inertial solvation time found in ethanol)[39] to a more relaxed excited state, from which intersystem crossing occurs (with a time constant of 39 ps) to yield the $T_1 \rightarrow T_n$ ESA (see Fig. S10 in ESI†). Although in this case no transient decay is assigned to conformational relaxation, at this point we cannot completely discard the occurrence of fast conformational relaxation in the sub-picosecond time regime (<1.6 ps).

## Conclusions

A comprehensive spectroscopic and photophysical study of oligoaniline derivatives (derived from arylamine and benzothiophene) has been undertaken in solution at 293 K and 77 K with the help of fast spectroscopic techniques. The effect of methyl and methoxy substitutions was shown to change some spectroscopic characteristics of these compounds. The increase in the number of methyl groups and the relative position (*ortho* and *meta* positions on the phenyl ring of aniline) of the methoxy groups in the benzo[*b*]thiophene core has shown to shift the fluorescence spectra. A charge transfer character of the singlet excited state was found for these compounds and this was supported by theoretical DFT calculations. From the photophysical characterization it was shown that the radiationless processes are the main excited state deactivation channels. In addition the ultrafast dynamics of the investigated compounds showed that the internal conversion and intersystem-crossing processes are the two main competitive decay channels in the singlet excited state deactivation.

## Acknowledgements

The authors thank the Fundação para a Ciência e Tecnologia (Portugal) and FEDER-COMPETE for financial support through the Coimbra Chemistry Centre (project UID/QUI/00313/2013). The FCT is acknowledged for a post-doctoral grant to J. Pina (ref. SFRH/BPD/108469/2015). The research leading to these results has received funding from Laserlab-Europe (grant agreement no. 284464, EC's Seventh Framework Programme).

## References

1 J. Seixas de Melo, L. M. Rodrigues, C. Serpa, L. G. Arnaut, I. Ferreira and M. Queiroz, Photochemistry and photophysics of thienocarbazoles, *Photochem. Photobiol.*, 2003, **77**, 121–128.

2 I. C. F. R. Ferreira, R. C. Calhelha, L. M. Estevinho and M.-J. R. P. Queiroz, Screening of antimicrobial activity of diarylamines in the 2,3,5-trimethylbenzo[*b*]thiophene series: a structure–activity evaluation study, *Bioorg. Med. Chem. Lett.*, 2004, **14**, 5831–5833.

3 A. S. Abreu, N. O. Silva, P. M. T. Ferreira, M. Queiroz and M. Venanzi, New β,β-bis(benzo [*b*]thienyl)dehydroalanine derivatives: Synthesis and cyclization, *Eur. J. Org. Chem.*, 2003, 4792–4796.

4 M. Queiroz, E. M. S. Castanheira, A. M. R. Pinto, I. Ferreira, A. Begouin and G. Kirsch, Synthesis of the first thieno-delta-carboline - Fluorescence studies in solution and in lipid vesicles, *J. Photochem. Photobiol., A*, 2006, **181**, 290–296.

5 A. S. Travis, *The rainbow makers - the origins of the synthetic dyestuffs industry in Western Europe*, Lehigh University Press, Bethlehem, 1993.

6 H. Zollinger, *Color Chemistry. Synthesis, Properties, and Applications of Organic Dyes and Pigments*, Verlag Helvetica Chimica Acta & Wiley-VCH, Zürich, 3rd edn, 2003.

7 M. E. Vaschetto and B. A. Retamal, Substituents effect on the electronic properties of aniline and oligoanilines, *J. Phys. Chem. A*, 1997, **101**, 6945–6950.

8 I. C. F. R. Ferreira, M.-J. R. P. Queiroz, M. Vilas-Boas, L. C. M. Estevinho, A. Begouin and G. Kirsch, Evaluation of the antioxidant properties of diarylamines in the benzo[*b*]-thiophene series by free radical scavenging activity and reducing power, *Bioorg. Med. Chem. Lett.*, 2006, **16**, 1384–1387.

9 A. G. McDiarmid and A. J. Epstein, *Faraday Discuss.*, 1989, **88**, 317.

10 S. Kapelle, W. Rettig and R. Lapouyade, Aniline dimers and trimers as model compounds for polyaniline: steric control of charge separation properties, *Chem. Phys. Lett.*, 2001, **348**, 416–424.

11 B. Wex, B. R. Kaafarani, E. O. Danilov and D. C. Neckers, Altering the Emission Behavior with the Turn of a Thiophene Ring: The Photophysics of Condensed Ring Systems of Alternating Benzenes and Thiophenes, *J. Phys. Chem. A*, 2006, **110**, 13754–13758.

12 J. P. Sadighi, R. A. Singer and S. L. Buchwald, Palladium-catalyzed synthesis of monodisperse, controlled-length, and functionalized oligoanilines, *J. Am. Chem. Soc.*, 1998, **120**, 4960–4976.

13 A. Gök, B. Sarı and M. Talu, Synthesis and characterization of conducting substituted polyanilines, *Synth. Met.*, 2004, **142**, 41–48.

14 R. A. Singer, J. P. Sadighi and S. L. Buchwald, A general synthesis of end-functionalized oligoanilines *via* palladium-catalyzed amination, *J. Am. Chem. Soc.*, 1998, **120**, 213–214.

15 I. C. F. R. Ferreira, M.-J. R. P. Queiroz and G. Kirsch, Synthesis of diarylamines in the benzo[*b*]thiophene series bearing electron donating or withdrawing groups by Buchwald–Hartwig C–N coupling, *Tetrahedron*, 2003, **59**, 975–981.

16 I. C. F. R. Ferreira, M.-J. R. P. Queiroz and G. Kirsch, Novel synthetic routes to thienocarbazoles *via* palladium or copper catalyzed amination or amidation of arylhalides and intramolecular cyclization, *Tetrahedron*, 2002, **58**, 7943–7949.
17 I. C. F. R. Ferreira, M.-J. R. P. Queiroz and G. Kirsch, Palladium-catalyzed amination and cyclization to heteroannellated indoles and carbazoles, *Tetrahedron*, 2003, **59**, 3737–3743.
18 R. S. Becker, J. Seixas de Melo, A. L. Maçanita and F. Elisei, Comprehensive evaluation of the absorption, photophysical, energy transfer, structural, and theoretical properties of alpha-oligothiophenes with one to seven rings, *J. Phys. Chem.*, 1996, **100**, 18683–18695.
19 S. Murov, I. Carmichael and G. L. Hug, *Handbook of Photochemistry*, M. Dekker Inc., New York, 1993.
20 J. Seixas de Melo, L. M. Silva and M. Kuroda, Photophysical and theoretical studies of naphthalene-substituted oligothiophenes, *J. Chem. Phys.*, 2001, **115**, 5625–5636.
21 J. Pina, J. Seixas de Melo, H. D. Burrows, A. L. Maçanita, F. Galbrecht, T. Bunnagel and U. Scherf, Alternating Binaphthyl-Thiophene Copolymers: Synthesis, Spectroscopy, and Photophysics and Their Relevance to the Question of Energy Migration *versus* Conformational Relaxation, *Macromolecules*, 2009, **42**, 1710–1719.
22 G. Striker, V. Subramaniam, C. A. M. Seidel and A. Volkmer, *J. Phys. Chem. B*, 1999, **103**, 8612.
23 G. Striker, Effective Implementation of Modulation Functions, in *Deconvolution and reconvolution of analytical signals*, ed. M. Bouchy, University Press, Nancy, 1982.
24 M. J. Frisch, G. W. Trucks, H. B. Schlegel, G. E. Scuseria, M. A. Robb, J. R. Cheeseman, G. Scalmani, V. Barone, B. Mennucci, G. A. Petersson, H. Nakatsuji, M. Caricato, X. Li, H. P. Hratchian, A. F. Izmaylov, J. Bloino, G. Zheng, J. L. Sonnenberg, M. Hada, M. Ehara, K. Toyota, R. Fukuda, J. Hasegawa, M. Ishida, T. Nakajima, Y. Honda, O. Kitao, H. Nakai, T. Vreven, J. A. Montgomery Jr., J. E. Peralta, F. Ogliaro, M. Bearpark, J. J. Heyd, E. Brothers, K. N. Kudin, V. N. Staroverov, R. Kobayashi, J. Normand, K. Raghavachari, A. Rendell, J. C. Burant, S. S. Iyengar, J. Tomasi, M. Cossi, N. Rega, J. M. Millam, M. Klene, J. E. Knox, J. B. Cross, V. Bakken, C. Adamo, J. Jaramillo, R. Gomperts, R. E. Stratmann, O. Yazyev, A. J. Austin, R. Cammi, C. Pomelli, J. W. Ochterski, R. L. Martin, K. Morokuma, V. G. Zakrzewski, G. A. Voth, P. Salvador, J. J. Dannenberg, S. Dapprich, A. D. Daniels, O. Farkas, J. B. Foresman, J. V. Ortiz, J. Cioslowski and D. J. Fox, *Gaussian 09, Revision A.02*, Gaussian, Inc., Wallingford CT, 2009.
25 A. D. Becke, A new mixing of Hartree–Fock and local density-functional theories, *J. Chem. Phys.*, 1993, **98**, 1372–1377.
26 M. M. Francl, W. J. Pietro, W. J. Hehre, J. S. Binkley, M. S. Gordon, D. J. Defrees and J. A. Pople, Self-consistent molecular-orbital methods 23. A polarization-type basis set for 2nd-row elements, *J. Chem. Phys.*, 1982, **77**, 3654–3665.
27 I. Carmichael and G. L. Hug, Triplet–Triplet Absorption-Spectra of Organic-Molecules in Condensed Phases, *J. Phys. Chem. Ref. Data*, 1986, **15**, 1–250.
28 H. D. Burrows, J. Seixas de Melo, C. Serpa, L. G. Arnaut, M. D. Miguel, A. P. Monkman, I. Hamblett and S. Navaratnam, Triplet state dynamics on isolated conjugated polymer chains, *Chem. Phys.*, 2002, **285**, 3–11.
29 M. Kristiansen, R. D. Scurlock, K. K. Iu and P. R. Ogilby, Charge-transfer state and singlet oxygen (1-delta-G O2) production in photoexcited organic-molecule molecular-oxygen complexes, *J. Phys. Chem.*, 1991, **95**, 5190–5197.
30 J. Pina, J. S. Seixas de Melo, A. Eckert and U. Scherf, Unusual photophysical properties of conjugated, alternating indigo-fluorene copolymers, *J. Mater. Chem. A*, 2015, **3**, 6373–6382.
31 J. Snellenburg, S. Laptenok, R. Seger, K. M. Mullen and I. H. M. Van Stokkum, *Glotaran: A Java-based graphical user interface for the R package TIMP*, *Journal of Statistical Software*, 2012, **49**, 1–22.
32 B. Valeur, *Molecular Fluorescence. Principles and Applications*, Wiley-VCH, Weinheim, 2002.
33 N. Turro, *Modern Molecular Photochemistry*, University Science Books, Sausalito, California, 1991.
34 J. Fabian, Electronic excitation of sulfur-organic compounds – performance of time-dependent density functional theory, *Theor. Chem. Acc.*, 2001, **106**, 199–217.
35 J. Fabian, L. A. Diaz, G. Seifert and T. Niehaus, Calculation of excitation energies of organic chromophores: a critical evaluation, *J. Mol. Struct. (THEOCHEM)*, 2002, **594**, 41–53.
36 T. Okamoto, K. Kudoh, A. Wakamiya and S. Yamaguchi, General Synthesis of Extended Fused Oligothiophenes Consisting of an Even Number of Thiophene Rings, *Chem. – Eur. J.*, 2007, **13**, 548–556.
37 B. Wardle, *Principles and Applications of Photochemistry*, Wiley, UK, 2009.
38 R. S. Becker, *Theory and Interpretation of Fluorescence and Phosphorescence*, Wiley-Interscience, New York, 1969.
39 M. L. Horng, J. A. Gardecki, A. Papazyan and M. Maroncelli, Subpicosecond Measurements of Polar Solvation Dynamics: Coumarin 153 Revisited, *J. Phys. Chem.*, 1995, **99**, 17311–17337.

 